Crystal Structure of Formycin 5′-Phosphate: An Explanation for Its Tight Binding to AMP Nucleosidase†

Vincent L. Giranda,‡,§ Helen M. Berman,*,‡ and Vern L. Schramm§,∥

Department of Biochemistry, Temple University School of Medicine, Philadelphia, Pennsylvania 19140, and Institute for Cancer Research, Fox Chase Cancer Center, Philadelphia, Pennsylvania 19111

Received December 21, 1987; Revised Manuscript Received April 11, 1988

ABSTRACT: Formycin 5′-monophosphate (FMP) is a strong competitive inhibitor of AMP nucleosidase with K_m/K_{is} from 1200 to 2600 depending on the source of the enzyme. The crystal structure of FMP has been determined in order to understand the basis for its high affinity for AMP nucleosidases and other biological properties. The key structural features of FMP are (1) the base is the N(7)–H tautomer, (2) the N(3) of the base forms an intramolecular hydrogen bond to the phosphate oxygen O(1), (3) the glycosyl torsion angle is syn with O(4′)–C(1′) relative to C(9)–C(4) being −6.43°, and (4) the furanose ring pucker is C(3′)-endo, with a pseudorotation angle of 20.3°. The major difference between the AMP and FMP structures is that the glycosyl torsion angles differ by 190°. The computed conformational energy necessary to distort AMP so that it has the same glycosyl torsion angle as FMP is 4.6 kcal/mol. This corresponds to a 2100-fold difference in binding energy, in good agreement with the observed interaction between AMP nucleosidase and FMP.

Formycin monophosphate (Figure 1) is formed by the monophosphorylation of formycin, a naturally occurring C-glycoside (Hori et al., 1964). The nucleoside formycin has been shown to have numerous biological and pharmacological properties. It inhibits the production of influenza virus (Takeuchi et al., 1966), suppresses synthesis of avian myeloblastosis cDNA, and suppresses synthesis of the rous sarcoma virus (Sarih et al., 1985). It is cytotoxic in neoplasms (Hori et al., 1964; Umezawa et al., 1967), and this cytotoxicity is enhanced by the addition of 2′-deoxycoformycin (Crabtree et al., 1981; Chu et al., 1981; Spemulli et al., 1983). To express its cytotoxicity, the formycin must first be phosphorylated to the monophosphate (Caldwell et al., 1966; Henderson et al., 1967).

The structure of formycin has been studied with X-ray crystallography (Prusiner et al., 1973; Koyama & Umezawa, 1974), NMR spectroscopy (Chenon et al., 1973; Krugh, 1973), ultraviolet absorption and emission spectroscopy (Ward & Reich, 1969; Wierzchowski & Shugar, 1982), temperature perturbations (Cole & Schimmel, 1978; Dodin et al., 1980), and molecular orbital modeling (Miles et al., 1974; Ceasar & Greene, 1974). Formycin is known to tautomerize between N(7)–H and N(8)–H forms (Chenon et al., 1979) and has a base protonation site, pK_a = 4.4 (Ward & Reich, 1969), thought to be N(3) in solution (Weirzchowski & Shugar, 1982). The results of the crystal structure analyses of the formycin nucleosides have shown they are in the syn configuration with C2′-endo furanose puckers. No crystal structure of formycin monophosphate has been reported to date.

Our main interest in formycin monophosphate's structure stems from its strong competitive inhibition of AMP nucleosides from *Escherichia coli* and *Azotobacter vinelandii*.

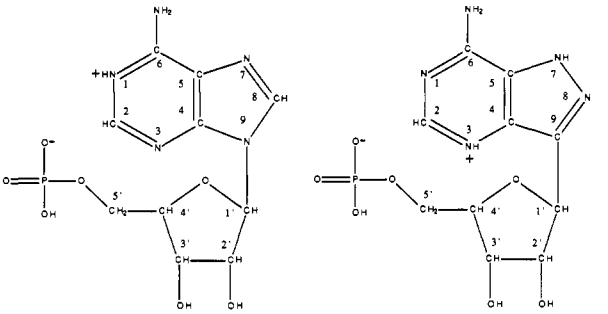

FIGURE 1: Structural formulas of formycin monophosphate (FMP) and adenosine monophosphate (AMP).

Formycin monophosphate binds 2600-fold more tightly to *A. vinelandii* AMP nucleosidase (DeWolf et al., 1979) and 1200-fold more tightly to *E. coli* AMP nucleosidase (Leung & Schramm, 1980) than the normal substrate, AMP. Formycin monophosphate binds to *A. vinelandii* AMP nucleosidase 120 times more tightly than formycin. It is thought that the inhibitory activity of formycin monophosphate is due primarily to its tendency to maintain a syn configuration about its *C*-glycosyl bond (DeWolf et al., 1979). In AMP nucleosidases are thought to induce considerable bond strain to the glycosyl bond during binding of substrate. It is postulated that this bond strain is caused by rotation of the base about the glycosyl bond. A complex between the *E. coli* AMP nucleosidase and formycin monophosphate has been crystallized and is currently being studied (Giranda et al., 1986).

Thus, the structure of formycin monophosphate is necessary to understand its biological properties, as well as its action as an AMP analogue in the AMP nucleosidase systems.

Materials and Methods

Crystal Growth and Characterization. Formycin monophosphate, free acid, was purchased from Calbiochem and was used without further purification. Crystallization was performed by slow evaporation of a saturated aqueous solution

† Support was provided by for H.M.B. by grants from NIH (GM21589, CA06927, and RR0559), for V.L.S. by a grant from NIH, (GM 21083), and for V.L.G. by a training grant from NIH (AM07163).

‡ Fox Chase Cancer Center.

§ Temple University School of Medicine.

∥ Present address: Department of Biochemistry, Albert Einstein College of Medicine, Bronx, NY 10461.

0006-2960/88/0427-5813$01.50/0

Table I: Crystal Data, Intensity Data Collection, and Refinement Parameters

molecular formula	$C_{10}H_{14}N_4O_7P \cdot 1.5H_2O$
formula weight	352.242
space group (monoclinic, No. 5)	$C2$
unit cell	
a (Å)	37.15(2)
b (Å)	4.750(2)
c (Å)	8.689(5)
β (deg)	95.16(4)
V (Å^3)	1527.2
Z (formula units per cell)	4
$F(000)$ (electrons)	676
μ (absorption coefficient) (cm^{-1})	20.29
data collection scan method	ω
2θ range (deg)	4.0–140.0
standard reflections (hkl)	(1,−1,−1), (−5,1,1), (0,2,0)
number of unique intensity data	1453
data with $I > 2\sigma(I)$	942
number of parameters refined	252
final $R = \sum(\|F_o\| - \|F_c\|)/\sum\|F_o\|$	0.067

of the free acid. After approximately 3 weeks small, colorless, needle-shaped crystals were formed (0.5 × 0.1 × 0.03 mm). Crystals were removed from the mother liquor and mounted on a glass fiber for X-ray analysis.

Initial characterization of the space group was performed with a General Electric sealed-tube generator. Cu Kα X-rays were used. Kodak DEF-5 film was used in a Charles Supper Weissenberg camera. The space group was determined from the systematically absent reflections $h + k = 2n + 1$. The unit cell specifications may be found in Table I.

X-ray Data Collection. Data collection was performed on an Enraf-Nonius-Delf CAD-4 automated diffractometer at 21 °C. The diffractometer was fitted with a graphite monochrometer and Cu Kα radiation, $\lambda = 1.54178$ Å, was used for the data collection.

The lattice constants were obtained by a least-squares method using the angular settings of 15 reflections with $2\theta = 18°–43°$. Data were collected from $\theta = 2°$ to $\theta = 70°$. The optimum scan was an ω scan, and the scan width was $2.0° + 0.15° \tan\theta$. Background measurements were taken on 25% of both sides of the ω scan. Each reflection was scanned for 10 s. Two octants of data were collected, $+h,+k,\pm l$. A total of 1453 nonredundant reflections were collected of which 942 were judged to be observed using the criterion $|F_o|^2 > 2(\sigma(I))$. These 942 data points were used in the solution and refinement of the structure. Three intensity standard reflections were measured after every 500 s of X-ray exposure time; no decay in these intensities could be observed. The data were corrected for Lorentz and polarization factors. No extinction correction was performed.

Structure Solution and Refinement. Patterson maps using all data and only data with $\sin\theta > 0.333$ were used to locate the phosphorus atom. Patterson map superposition was then performed to locate the oxygens of the phosphate group. The rest of the non-hydrogen atoms were located by Fourier methods. The structure was refined by the method of least squares. The value which was minimized was $\sum w(\Delta F^2)$, where $\Delta F = |F_o| - |F_c|$ and $w = k/\sigma^2$. The value for k was obtained by minimizing the function $|\Delta F|^2 - \sigma^2/k$, where $\sigma = \sigma(I)/\sqrt{I}$. The structure was refined one cycle on the scale factor only, then two cycles isotropically, and then three cycles anisotropically. Hydrogens were located by difference electron density maps. Only 10 of the 17 hydrogens in the asymmetric unit could be unambiguously located in this manner. The small size of the crystal and consequent weak intensities probably contributed to the inability to locate all of the hydrogen atoms. These ten hydrogens were placed in the model, and the model

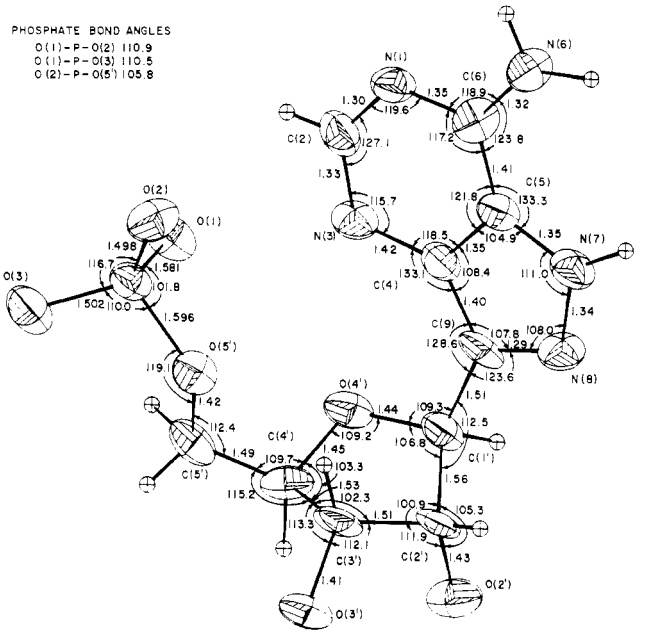

FIGURE 2: Bond angles and distances for formycin monophosphate. The standard deviations for bonds and angles involving phosphorus are 0.007 Å and 0.5°. For all other non-hydrogen atoms the standard deviations in bond lengths and angles are 0.01 Å and 0.7°.

was refined for two more cycles. The hydrogens were refined isotropically, and the non-hydrogen atoms were refined anisotropically during these final two cycles of refinement. The final R factor for the observed data is 0.067. A summary of the data collection and structure solution is given in Table I.

Results

Formycin monophosphate is a AMP analogue which has a nitrogen in position 8 and a carbon in position 9 of the base (Figure 1). The atomic positions and thermal parameters for formycin monophosphate are found in Table II. The bond lengths and angles of formycin monophosphate are pictured in Figure 2. The major features of the formycin monophosphate structure are that the base is syn with respect to the sugar, there is an intramolecular hydrogen bond between the phosphate and the base, and the formycin monophosphate is zwitterionic with the phosphate carrying the negative charge and the base carrying the positive charge.

Pyrasolopyrimidine Base Structure. The base is nearly planar, with the largest deviation from the plane of 0.0023 Å at C(9). The base is known to tautomerize between the N(7)–H and N(8)–H forms in solution (Chenon et al., 1973). In this structure the base is the N(7)–H tautomer. The data which support the N(7)–H tautomer are as follows: the difference Fourier maps showed the hydrogen atom at position N(7) and not at N(8); N(7) must act as a hydrogen donor in the only plausible hydrogen-bonding scheme; and the geometry of the base is consistent with the N(7)–H tautomer. When the two forms are compared crystallographically, it has been shown that decreases in the C(4)–C(5) and N(8)–C(9) bond lengths and N(7)–N(8)–C(9) and N(7)–C(5)–C(4) bond angles can be expected in the N(7)H tautomer (Koyama & Umezawa, 1974). Also expected in the N(7)H tautomer are increases in the C(5)–C(6) and C(9)–C(4) bond lengths and N(7)–C(5)–C(6), C(4)–C(9)–N(8), and N(8)–N(7)–C(5) bond angles. With the exception of the C(4)–C(9)–N(8) bond angle, all of the bond lengths and angles in the FMP structure are consistent with it being an N(7)H tautomer.

The base can be protonated at one of two sites, N(1) or N(3). In solution the predominant site of protonation is N(3)

Table II: Atomic Positions with Estimated Standard Deviations and Thermal Parameters with Estimated Standard Deviations for Formycin Monophosphate[a]

(A) Atomic Positions and Isotropic Thermal Parameters for Formycin Monophosphate

atom	x	y	z	B (Å^3)	atom	x	y	z	B (Å^3)
P(1)	0.32616 (6)	0.7000 (0)	0.2142 (3)	2.60	C(6)	0.2920 (2)	0.258 (1)	0.7740 (10)	2.83
O(1)	0.3170 (2)	0.952 (1)	0.3232 (8)	3.66	N(6)	0.2753 (2)	0.065 (2)	0.8510 (10)	3.60
O(2)	0.3016 (2)	0.455 (1)	0.2334 (8)	3.81	N(7)	0.3562 (2)	0.209 (2)	0.8975 (8)	3.18
O(3)	0.3288 (2)	0.803 (1)	0.0523 (7)	3.82	N(8)	0.3880 (2)	0.332 (2)	0.8763 (9)	3.17
C(1′)	0.4120 (2)	0.689 (2)	0.7051 (9)	2.92	C(9)	0.3824 (2)	0.512 (2)	0.7650 (10)	2.77
C(2′)	0.4435 (2)	0.507 (2)	0.6530 (10)	2.85	W(1)	0.0509 (2)	0.753 (2)	0.8970 (10)	7.26
C(3′)	0.4329 (2)	0.485 (2)	0.4820 (10)	3.07	W(2)	0.5000 (0)	0.871 (2)	0.0000 (0)	6.26
C(4′)	0.4179 (2)	0.780 (2)	0.4430 (10)	2.81	C(1′)H	0.423 (2)	0.79 (2)	0.810 (10)	4.49
C(5′)	0.3940 (2)	0.800 (2)	0.2950 (10)	3.38	C(2′)H	0.447 (3)	0.36 (2)	0.700 (10)	3.08
O(2′)	0.4754 (1)	0.675 (2)	0.6858 (7)	3.94	C(3′)H	0.408 (3)	0.36 (2)	0.450 (10)	5.40
O(3′)	0.4624 (1)	0.412 (1)	0.3986 (7)	3.33	C(4′)H	0.444 (2)	0.91 (2)	0.440 (10)	3.06
O(4′)	0.3975 (1)	0.845 (1)	0.5718 (7)	3.04	C(5′)H(1)	0.379 (2)	1.03 (2)	0.270 (10)	2.50
O(5′)	0.3650 (2)	0.605 (1)	0.2894 (7)	2.95	C(5′)H(2)	0.405 (2)	0.77 (2)	0.205 (9)	0.41
N(1)	0.2730 (2)	0.404 (2)	0.6615 (9)	3.04	C(2)H	0.277 (2)	0.70 (2)	0.510 (10)	2.63
C(2)	0.2891 (3)	0.594 (2)	0.5850 (10)	3.44	N(6)H(1)	0.252 (2)	0.04 (2)	0.821 (9)	1.44
N(3)	0.3240 (2)	0.659 (2)	0.5999 (8)	3.01	N(6)H(2)	0.283 (2)	−0.07 (2)	0.935 (8)	0.77
C(4)	0.3454 (2)	0.510 (2)	0.7160 (10)	2.87	N(7)H	0.352 (3)	0.07 (2)	0.970 (10)	4.22
C(5)	0.3294 (2)	0.315 (2)	0.7990 (10)	3.09					

(B) Anisotropic Thermal Parameters for Formycin Monophosphate

atom	β_{11}	β_{22}	β_{33}	β_{12}	β_{13}	β_{23}
P(1)	0.00050 (1)	0.0258 (8)	0.0099 (3)	0.0008 (2)	0.00110 (9)	0.005 (1)
O(1)	0.00083 (5)	0.032 (3)	0.0135 (10)	0.0007 (7)	0.0023 (4)	0.003 (3)
O(2)	0.00052 (4)	0.035 (3)	0.0175 (10)	0.0002 (6)	−0.0004 (4)	0.006 (3)
O(3)	0.00085 (5)	0.046 (3)	0.0102 (9)	0.0012 (7)	0.0019 (3)	0.004 (3)
C(1′)	0.00058 (6)	0.034 (4)	0.0097 (10)	0.0020 (10)	0.0020 (4)	0.007 (4)
C(2′)	0.00039 (5)	0.045 (5)	0.0096 (10)	0.0012 (8)	0.0025 (4)	0.005 (4)
C(3′)	0.00046 (5)	0.040 (5)	0.0125 (10)	0.0039 (9)	0.0031 (5)	0.006 (4)
C(4′)	0.00036 (5)	0.024 (4)	0.0147 (10)	−0.0002 (7)	0.0007 (4)	−0.015 (4)
C(5′)	0.00078 (7)	0.033 (4)	0.0112 (10)	−0.0025 (9)	0.0022 (5)	0.011 (4)
O(2′)	0.00045 (4)	0.049 (3)	0.0165 (10)	−0.0010 (7)	0.0004 (3)	−0.012 (3)
O(3′)	0.00052 (4)	0.039 (3)	0.0140 (10)	0.0009 (6)	0.0027 (3)	−0.005 (3)
O(4′)	0.00051 (4)	0.031 (3)	0.0131 (9)	0.0009 (6)	0.0018 (3)	0.000 (3)
O(5′)	0.00064 (5)	0.022 (3)	0.0115 (9)	0.0000 (5)	0.0007 (3)	0.003 (2)
N(1)	0.00043 (5)	0.034 (4)	0.0130 (10)	0.0007 (7)	0.0010 (4)	0.013 (3)
C(2)	0.00074 (8)	0.046 (5)	0.0078 (10)	0.0014 (10)	0.0012 (5)	−0.001 (4)
N(3)	0.00044 (4)	0.035 (4)	0.0118 (10)	−0.0039 (7)	0.0004 (3)	−0.003 (3)
C(4)	0.00055 (6)	0.037 (5)	0.0085 (10)	0.0015 (9)	0.0014 (5)	0.007 (4)
C(5)	0.00047 (6)	0.045 (5)	0.0096 (10)	0.0001 (9)	0.0009 (4)	−0.001 (4)
C(6)	0.00062 (6)	0.008 (4)	0.014 (10)	0.0005 (7)	−0.0003 (5)	0.001 (3)
N(6)	0.00050 (5)	0.033 (3)	0.0165 (10)	−0.0021 (7)	−0.0005 (5)	0.028 (4)
N(7)	0.00052 (5)	0.039 (4)	0.0111 (10)	−0.0028 (9)	0.0011 (4)	0.005 (4)
N(8)	0.00040 (4)	0.034 (4)	0.0141 (10)	−0.0028 (7)	0.0000 (4)	0.008 (4)
C(9)	0.00060 (6)	0.033 (4)	0.0087 (10)	0.0011 (9)	0.0028 (5)	−0.002 (4)
W(1)	0.00111 (6)	0.109 (6)	0.0181 (10)	−0.0093 (10)	−0.0017 (5)	0.031 (5)
W(2)	0.00134 (10)	0.049 (6)	0.0254 (30)	0.0000 (0)	0.0030 (9)	0.000 (0)

[a] Thermal parameters are in the form $\exp[-(\beta_{11}h^2 + \beta_{22}k^2 + \beta_{33}l^2 + 2\beta_{12}hk + 2\beta_{13}hl + 2\beta_{23}kl)]$.

(Weirzchowski & Shugar, 1982). Although the data are inconclusive, because difference Fourier maps could not locate hydrogens at either the N(3) or N(1) sites, the data support that crystalline formycin monophosphate is protonated at N(3). In agreement with N(3) protonation is that the C(2)–N(3)–C(4) bond angle is widened by 3.2° in formycin monophosphate when compared to that in neutral formycin monohydrate. Additional support for N(3) protonation is that N(3) should be a hydrogen donor in a hydrogen bond with O(1) of the phosphate. N(3) must be a hydrogen donor; otherwise, only one of two possible hydrogen bonds to O(1) could exist.

In formycin monophosphate, the geometry of the base does not support protonation at N(1). The most consistent change seen in N(1) protonation is the widening of the C(2)–N(1)–C(6) angle. Other changes include lengthening of the N(1)–C(6) and N(1)–C(2) bonds, shortening of the C(2)–N(3) and C(6)–N(6) bonds, and narrowing of the N(1)–C(6)–C(5) and N(1)–C(2)–N(3) angles (Prusiner et al., 1973). Formycin hydrobromide monohydrate which is protonated at N(1) has these geometrical features, whereas the unprotected formycin monohydrate does not.

Furanose Ring. The furanose ring of formycin monophosphoric acid is in the C(3′)-endo form with a pseudorotation angle $P = 20.3$ (Altona & Sundaralingam, 1972). As shown in Table III the furanose ring conformation differs significantly from those in the formycin nucleosides. Both formycin nucleoside crystal structures had demonstrated a C(2′)-endo furanose ring pucker. The C(3′)-endo furanose ring pucker of formycin monophosphate is similar to that found in the crystal structure of AMP (Kraut & Jensen, 1963).

O(4′)–C(1′)–C(9)–C(4) Torsion Angle. The glycosyl torsion angle in formycin monophosphate is in the syn conformation with an O(4′)–C(1′)–C(9)–C(4) torsion angle of −6.43°. Formycin and formycin B nucleoside crystal structures solved include formycin monohydrate (Prusiner et al., 1973), formycin hydrobromide monohydrate (Koyama et al., 1974), 2-methylformycin (Abola et al., 1973), formycin B hydrochloride (Singh & Hodgson, 1977), formycin B, and oxoformycin B (Koyama et al., 1976). All of these structures except formycin B and formycin monohydrate have *syn*-glycosyl torsion angles which are stabilized via an intramolecular hydrogen bond between O(5′) and N(3). As shown in Table III there are large differences between the glycosyl

Table III: Selected Torsion Angles from FMP, AMP, Formycins, and Formycins B

compound	pseudorotation[a]	angles (deg) O(1')–C(1')–C(9)–C(4)	C(3')–C(4')–C(5')–O(5')	C(4')–C(5')–O(5')–P
formycin monophosphate	20.3, C(3')-endo	−6.43 (syn)	141.3	54.1
AMP[b]	12.2, C(3')-endo	−163.92 (anti)	177.2	40.0
formycin monohydrate[c]	148.3, C(2')-endo	−73.83 (high anti)	175.8	
formycin hydrobromide monohydrate[d]	177.0, C(2')-endo	34.50 (syn)	162.3	
2-methylformycin[e]	C(3')-endo	−25.20 (syn)		
formycin B[f]	143.3, C(2')-endo	−155.16 (anti)	55.9	
formycin B hydrochloride[g]	154.8, C(2')-endo	43.31 (syn)	59.2	
oxoformycin B[f]	30.8, C(3')-endo	18.11 (syn)	59.9	

[a] The pseudorotation angle is as defined in Altona and Sundaralingam (1971). [b] Data from Kraut and Jensen (1963). [c] Data from Prusiner et al. (1973). [d] Data from Koyama et al. (1974). [e] Data from Abola et al. (1973). [f] Data from Koyama et al. (1976). [g] Data from Singh & Hodgson (1977).

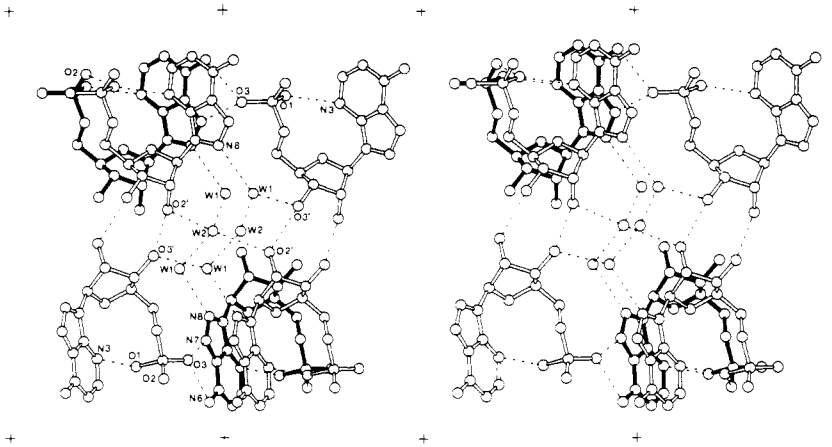

FIGURE 3: A stereo diagram of the crystal structure and hydrogen-bonding scheme of formycin monophosphate. All hydrogen atoms have been left out of the diagram for clarity. The molecules illustrated with shaded bonds are translated one unit cell along the *b* axis behind the unshaded molecules nearest them. The hydrogen bonds are illustrated as dashed lines. The water molecule, W2, lies on a twofold axis.

angles of the formycin nucleosides and those of FMP and AMP. There is a 190° difference in these angles in formycin monophosphate and in adenosine monophosphate. The glycosyl torsion angle of near zero in the structure of formycin monophosphate in stabilized by the intramolecular hydrogen bond between the phosphate oxygen, O(1), and N(3) of the formycin base, rather than by an O(5')···N(3) hydrogen bond as found in formycin nucleosides.

Phosphate. The P–O bond lengths and the O–P–O bond angles are all consistent with observations of 15 monoester monoanions (Saenger, 1984). These lengths and angles indicate that O(1) is covalently bound to a hydrogen and that the phosphate oxygens, O(2) and O(3), carry the negative charge.

The torsion angles about the C(4')–C(5') and C(5')–O(5') bonds are such that O(1) of the phosphate is in a position to form an intramolecular hydrogen bond with N(3) of the base. The O(5')–C(5')–C(4')–C(3') torsion angle is 54.41°. The C(4')–C(5') bond is in the gauche,gauche configuration, +sc (Saenger, 1984). The C(4')–C(5')–O(5')–P torsion angle is 141.3°.

Crystal Structure (Figure 3). There are four formycin monophosphate molecules and six H_2O molecules per unit cell. One of the H_2O molecules [W(2)] lies on a twofold axis in the unit cell. Bases do not stack directly on top of each other; rather, the N(2)–C(3)–C(4)–C(9) edge of one base lies near the C(6)–C(5)–N(7) edge of an adjacent base. The closest contacts between bases are as follows: C(2) to N(6), 3.28 Å; N(3) to C(6), 3.48 Å; C(3) to N(6), 3.52 Å; N(1) to N(6), 3.54 Å; C(2) to C(6), 3.56 Å; N(3) to C(5), 3.56 Å; N(7) to C(9), 3.66 Å; C(5) to C(9), 3.68 Å. Each formycin monophosphate participates in 13 intermolecular hydrogen bonds which act to stabilize the crystal structure (Table IV).

Table IV: Hydrogen-Bonding Distances and Estimated Standard Deviations between Non-Hydrogen Atoms[a]

hydrogen bond	distance (ESD) (Å)	hydrogen bond	distance (ESD) (Å)
O(1)···N(3)	2.767 (10)	O(1)···O(2)	2.561 (9)
O(2)···N(6)	2.932 (9)	O(3)···N(6)	2.818 (10)
O(3)···N(7)	2.608 (10)	O(2')···O(3')	2.782 (8)
O(2')···W(2)	2.782 (7)	O(3')···W(1)	2.683 (11)
N(8)···W(1)	2.891 (10)	W(1)···W(2)	2.825 (12)

[a] The O(1)···N(3) hydrogen bond is intramolecular; all others are intermolecular.

The water molecules form a channel along the twofold axis. The water molecules and the furanose hydroxyl moieties from a spiraling network of hydrogen bonds. Because the hydrogens in these bonds could not be located on difference Fourier maps, two possible hydrogen-bonding schemes are possible:

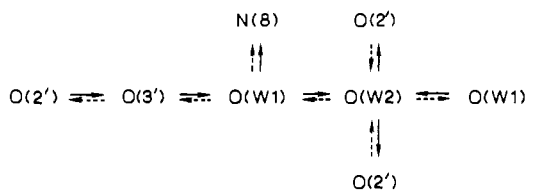

The solid lines with arrows indicate one hydrogen-bonding scheme, and the dashed lines indicate the alternate scheme. This possibility for disorder may contribute to the difficulty in locating these hydrogens on difference Fourier maps. Figure 3 shows the spatial arrangement of this hydrogen-bonding network.

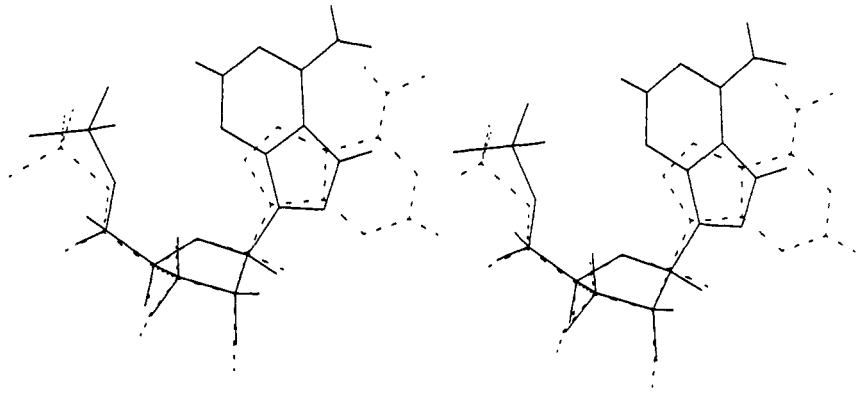

FIGURE 4: A stereo diagram comparing the structure of formycin monophosphate (solid) and AMP (dashed). The ribose rings of both structures were kept isosteric in this diagram.

The phosphate hydrogen-bonding clusters about a 2_1 screw axis. Each phosphate is hydrogen bonded to three separate formycin monophosphate molecules. The O(1) of the phosphate is within hydrogen-bonding distance of both the N(3) of the same molecule and the O(2) of a neighboring molecule. Since O(1) is known to carry the hydrogen of the phosphate group and O(2) is known not to carry a hydrogen, the only possible way for O(1) to be hydrogen bonded to both N(3) and O(2) is for N(3) to act as a hydrogen donor. The phosphate O(2) is also hydrogen bonded to N(6)H(1) of a neighboring molecule. The O(3) phosphate oxygen is hydrogen bonded to both N(7)H and N(6)H(2) of a neighboring formycin monophosphate. No hydrogens of the phosphate group could be located by the difference Fourier maps.

Discussion

Several structural features of formycin monophosphate are unusual for nucleotide analogues. It is rare for a nucleotide to show a syn configuration about the glycosyl bond. It is even less common for these nucleotides in the syn configuration to have a C(3′)-endo furanose ring pucker (Saenger, 1984) as does formycin monophosphate. A notable exception is deoxyguanosine in Z-DNA (Wang et al., 1979).

The conformations in FMP are different from those of AMP and the two formycin nucleosides reported to date (Table III). As illustrated in Figure 4, there are two outstanding differences between the crystal structures of formycin monophosphate and AMP. In formycin monophosphate the C(4′)–C(5′)–O(5′)–P torsion angle is 141° whereas in AMP it is 177°. This difference allows the phosphate oxygen in formycin monophosphate, O(1), to come within hydrogen-bonding distance of the N(3) of the formycin base. The major difference between the formycin monophosphate and AMP structures is the conformation about the glycosyl bond; it is anti in AMP and syn in FMP.

The structure of formycin monophosphate provides an explanation for its a strong competitive inhibition of AMP nucleosidase. The enzyme is thought to induce bond strain on the substrate AMP by rotation about the glycosyl bond (DeWolf et al., 1979). Catalysis features a transition-state structure in which the ribose monophosphate has strong oxycarbonium character (Mentch et al., 1987). Strain at the glycosyl bond would be a rational step in the formation of an oxycarbonium-like transition state. The hypothesis to be tested proposes that binding of AMP to the catalytic site of AMP nucleosidase involves rotation around the glycosyl bond to a position similar to that of formycin monophosphate. The relatively tight binding of formycin monophosphate can be explained by assuming that the energy required for conformational distortion of the substrate is converted into binding energy for formycin monophosphate, since its conformation is solution conforms to the substrate binding site.

The glycosyl torsion angle in the structure of formycin monophosphate may provide an estimate of the transition-state conformation of the enzyme-bound substrate molecule. The binding energy used to distort the glycosyl bond of the substrate can then be estimated by referring to the computed conformational energies of AMP in a configuration approaching that of formycin monophosphate. For AMP to be distorted to the same glycosyl torsion conformation as formycin monophosphate, 4.6 kcal/mol of energy is necessary (Yathindra & Sundaralingam, 1973). This corresponds to a 2100-fold preference for AMP nucleosidase to bind a molecule with a conformation like that of formycin monophosphate. This figure is in good agreement with the experimentally derived values for the binding of formycin monophosphate. This K_m/K_{is} ratio for AMP/formycin monophosphate is 2600 for AMP nucleosidase from *A. vinelandii* and 1200 for AMP nucleosidase from *E. coli* (DeWolf et al., 1979; Leung & Schramm, 1980).

In AMP, N(1) is the preferred protonation site for the adenine ring, rather than N(3) as found in formycin 5′-phosphate. However, N(3) could still participate in hydrogen-bond formation with a phosphate hydroxyl group of enzyme-bound AMP. If AMP is moved into a formycin monophosphate like configuration, only slight conformational changes are necessary to allow a bifurcated hydrogen bond to form from a phosphate OH to both N(3) of AMP and O(4′) or ribose 5-phosphate. Such an interaction would be expected to stabilize the developing oxycarbonium intermediate.

The tautomeric form of formycin monophosphate involves protonation of N(7). In AMP, protonation of N(7) is difficult with a pK_a near 1.0, although protonation of this group is proposed to occur in the formation of the transition state (Mentch et al., 1987). The difference in pK_a's might also explain the tight binding of formycin monophosphate. Direct comparison of the pK_a profiles for the K_m for AMP and the K_{is} for formycin monophosphate gave overlapping curves (DeWolf et al., 1986). Thus no differences in ionizable groups appear to be influencing AMP or formycin monophosphate binding over the range of pHs from 5 to 9. These results again implicate the glycosyl torsion structue as the major difference responsible for the relative tight binding of formycin monophosphate to AMP nucleosidases.

Acknowledgments

We thank Steve Ginell and Pat Sawzik for their helpful suggestions. We also thank the reviewer for suggesting that

a bifurcated hydrogen bond may exist in enzyme-bound AMP.

Supplementary Material Available

FMP observed and unobserved calculated structure factors (9 pages). Ordering information is given on any current masthead page.

References

Abola, J. E., Sims, M. J., & Abraham, D. J. (1974) *J. Med. Chem. 17*, 62–65.

Altona, C., & Sundaralingam, M. (1971) *J. Am. Chem. Soc. 94*, 8205–8212.

Caldwell, I. C., Henderson, J. F., & Patterson, A. R. P. (1966) *Proc. Am. Assoc. Cancer Res. 7*, 11.

Ceasar, G. P., & Greene, J. J. (1974) *J. Med. Chem. 17*, 1122–1124.

Chenon, M. T., Pugmire, R. J., Grant, D. M., Panzica, R. P., & Townsend, L. B. (1973) *J. Heterocycl. Chem. 10*, 431–433.

Chu, M. Y., Bogden, A. E., Wiemann, M. C., Cummings, F. J., Bogaars, H., & Calabresi, P. (1981) *Proc. Am. Assoc. Cancer Res. 22*, 231.

Cole, F. X., & Schimmel, P. R. (1978) *J. Am. Chem. Soc. 100*, 3957–3958.

Crabtree, G. W., Dexter, D. L., Spremulli, E. N., Quevedo W. C., Jr., Calabresi, P., & Parks, R. E., Jr. (1981) *Proc. Am. Assoc. Cancer Res. 22*, 250.

DeWolf, W. E., Fullin, F. A., & Schramm, V. L. (1979) *J. Biol. Chem. 254*, 10868–10875.

DeWolf, W. E., Fullin, F. A., & Schramm, V. L. (1986) *Biochemistry 25*, 4132–4140.

Dodin, G., Bensaude, O., & Dubois, J. (1980) *J. Am. Chem. Soc. 102*, 3897–3899.

Giranda, V. L., Berman, H. M., & Schramm, V. L. (1986) *J. Biol. Chem. 261*, 15307–15309.

Henderson, J. F., Patterson, A. R. P., Caldwell, I. C., & Hori, M. (1967) *Cancer Res. 27*, 715–719.

Hori, M., Ito, E., Takita, T., Koyama, G., Takeuchi, T., & Umezawa, H. (1964) *J. Antibiot., Ser. A 17*, 96–99.

Koyama, G., Umezawa, H., & Iitaka, Y. (1974) *Acta Crystallogr., Sect. B: Struct. Crystallogr. Cryst. Chem. B30*, 1511–1516.

Koyama, G., Nakamura, H., Umezawa, H., & Iitaka, Y. (1976) *Acta Crystallogr., Sect. B: Struct. Crystallogr. Cryst. Chem. B32*, 813–820.

Kraut, J., & Jensen, L. H. (1963) *Acta Crystallogr. 16*, 79–88.

Krugh, T. R. (1973) *J. Am. Chem. Soc. 95*, 4761–4762.

Leung, H. B., & Schramm, V. L. (1980) *J. Biol. Chem. 255*, 10867–10874.

Mentch, F., Parkin, D. W., & Schramm, V. L. (1987) *Biochemistry 26*, 921–930.

Miles, D. W., Miles, D. L., & Eyring, H. (1974) *J. Theor. Biol. 45*, 577–583.

Prusiner, P., Brennan, T., & Sundaralingam, M. (1973) *Biochemistry 12*, 1196–1201.

Saenger W. (1984) in *Principles of Nucleic Acid Structure* (Cantor, C. R., Ed.) pp 23–24, 69, 82–88, Springer-Verlag, New York.

Sarih, L., Agoutin, B., Lecoq, O., Weill, D., Jullien, P., & Heyman, T. (1985) *Virology 145*, 171–175.

Singh, P., & Hodgson, D. J. (1977) *Acta Crystallogr., Sect. B: Struct. Crystallogr. Cryst. Chem.*

Spemulli, E. N., Crabtree, G. W., Dexter, D. L., Chu, S. H., Farineau, D. M., Ghoda, L. Y., McGowan, D. L., Diamond, I., Parks, R. E., Jr., & Calabresi, P. (1983) *Can. Treat. Rep. 67*, 267–274.

Takeuchi, T., Iwanaga, J., Aoyagi, T., & Umezawa, H. (1966) *J. Antibiot., Ser. A. 19*, 286–289.

Umezawa, H., Sawa, T., Fukagawa, Y., Homma, I., Ishizuka, M., & Takeuchi, T. (1967) *J. Antibiot. Ser. A. 20*, 308–316.

Wang, A. H.-J., Quigley, F. J., Kolpak, F. J., Crawford, J. L., van Boom, J. H., van der Marel, G., & Rich, A. (1979) *Nature (London) 282*, 680–686.

Ward, D. C., & Reich, E. (1969) *J. Biol. Chem. 244*, 1228–1237.

Wierzchowski, J., & Shugar, D. (1982) *Photochem. Photobiol. 35*, 445–458.

Yathindra, N., & Sundaralingam, M. (1973) *Biopolymers 12*, 297–314.